Progress in Natural Science: Materials International 2013;23(3):343–350

Chinese Materials Research Society

Progress in Natural Science: Materials International

www.elsevier.com/locate/pnsmi
www.sciencedirect.com

LETTERS

Facile synthesis of nanosized sodium magnesium hydride, $NaMgH_3$

Hazel Reardon[a], Natalia Mazur[a,b], Duncan H. Gregory[a,*]

[a]*WestCHEM, School of Chemistry, Joseph Black Building, University of Glasgow, Glasgow G12 8QQ Scotland, UK*
[b]*Department of Materials Science and Engineering, Norwegian University of Science and Technology, N-7491 Trondheim, Norway*

Received 11 September 2012; accepted 25 March 2013
Available online 2 June 2013

KEYWORDS

Hydride;
Mechanochemistry;
Structure;
Hydrogen storage;
Raman

Abstract The ternary magnesium hydride $NaMgH_3$ has been synthesised *via* reactive milling techniques. The method employed neither a reactive H_2 atmosphere nor high pressure sintering or other post-treatment processes. The formation of the ternary hydride was studied as a function of milling time and ball:powder ratio. High purity $NaMgH_3$ powder (orthorhombic space group *Pnma*, $a=5.437(2)$ Å, $b=7.705(5)$ Å, $c=5.477(2)$ Å; $Z=4$) was prepared in 5 h at high ball:powder ratios and characterised by powder X-ray diffraction (PXD), Raman spectroscopy and scanning electron microscopy/energy dispersive X-ray spectroscopy (SEM/EDX). The products formed sub-micron scale (typically 200–400 nm in size) crystallites that were approximately isotropic in shape. The dehydrogenation behaviour of the ternary hydride was investigated by temperature programmed desorption (TPD). The nanostructured hydride releases hydrogen in two steps with an onset temperature for the first step of 513 K.

1. Introduction

Ternary hydrides are of significant importance in the development of candidate hydrogen storage systems. The hydrides of magnesium are of particular interest given the potential for high capacity, low cost materials [1]. Extensive reviews by Yvon and co-workers describe an array of ternary and quaternary hydride compounds containing combinations of alkali, alkaline earth and transition metals. Synthesis of such compounds typically requires the high pressure sintering of respective metals/metal hydrides or alloys [2,3]. Mechanical modification of metals and their hydrides has been shown to improve hydrogen sorption characteristics *via* the introduction of enhanced surface characteristics and morphologies (e.g. defects, increased surface area, increased surface:volume ratios). Significant reduction of particle sizes to the nanoscale can improve not only the kinetics but also the thermodynamics of hydrogen uptake and release [4–6].

Among possible complex hydrides, ABH_3 perovskites (where A is usually an alkali or alkaline earth metal and B is a transition metal) are being considered as strong competitors to nanoscale AH_2-type

*Corresponding author. Tel.: +44 141 3306438; fax: +44 141 3308333.
E-mail address: Duncan.Gregory@glasgow.ac.uk (D.H. Gregory).
Peer review under responsibility of Chinese Materials Research Society.

ELSEVIER Production and hosting by Elsevier

1002-0071 © 2013 Chinese Materials Research Society. Production and hosting by Elsevier B.V. All rights reserved.
http://dx.doi.org/10.1016/j.pnsc.2013.05.003

hydrides [7,8]. Replacement of transition metals (B) with early alkali/alkaline earth metals in ABH_3 compounds maximises potential gravimetric capacity and computational studies have shown that such high capacity hydrides may exist ($LiMgH_3$ and Li_2MgH_4 contain 8.84 and 9.57 wt% H_2, respectively) [9,10]. These compounds, however, are yet to be realised experimentally. $KMgH_3$ has been extensively studied, both experimentally and computationally [9–18]. Both solid state and mechanochemistry techniques have been employed to prepare $KMgH_3$ and desorption of hydrogen from the hydride occurs in one step. $NaMgH_3$ may be synthesised *via* reactive mechanochemical means. Use of 1 MPa (10 bar) H_2 during milling of a 1:1 NaH:MgH_2 mixture formed the hydride, which displayed an experimental capacity of 5.8 wt% H (*cf.* a theoretical capacity of 6.0 wt%) [13,19]. Prior to this work, the synthesis of $NaMgH_3$ involved reaction of the hydrides at 480 °C under 10 bar of hydrogen [20,21]. Cryo-milling of the binary hydrides with subsequent high pressure H_2 sintering treatments has also been employed [22–24]. Indeed, mechanochemical approaches provide not only less energy intensive routes to the hydrides, but also ensure that particles sizes are minimised, improving the dehydrogenation kinetics of the ternary hydrides compared to those prepared at high temperature [25,26]. There is a growing interest in $NaMgH_3$ and related hydrides and a drive to understand the sorption mechanisms in these systems in more detail by both experimental and computational methods [27–33]. Here we describe the facile mechanochemical synthesis of nanoscale $NaMgH_3$ without a requirement for hydrogen during milling. Using a combination of characterisation techniques, we report the influence of milling times and parameters both on the progress of the mechanochemical reaction and on the identity and properties of the products.

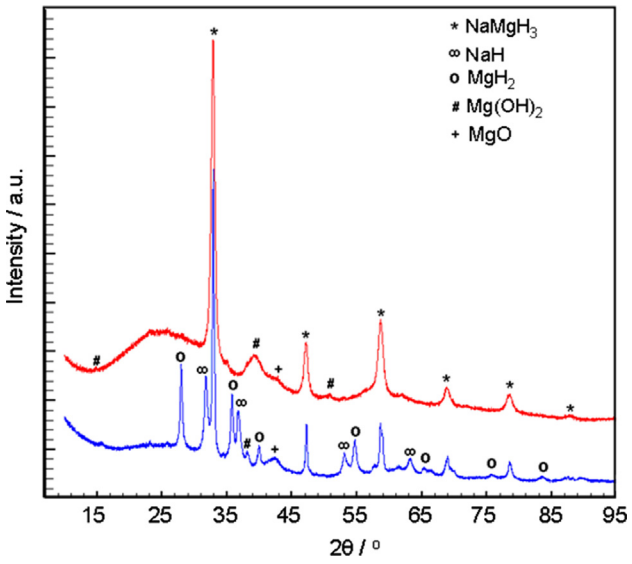

Fig. 1 NaH and MgH_2 milled for 1 h (blue) and 5 h (red) (with a b:p of 70:1).

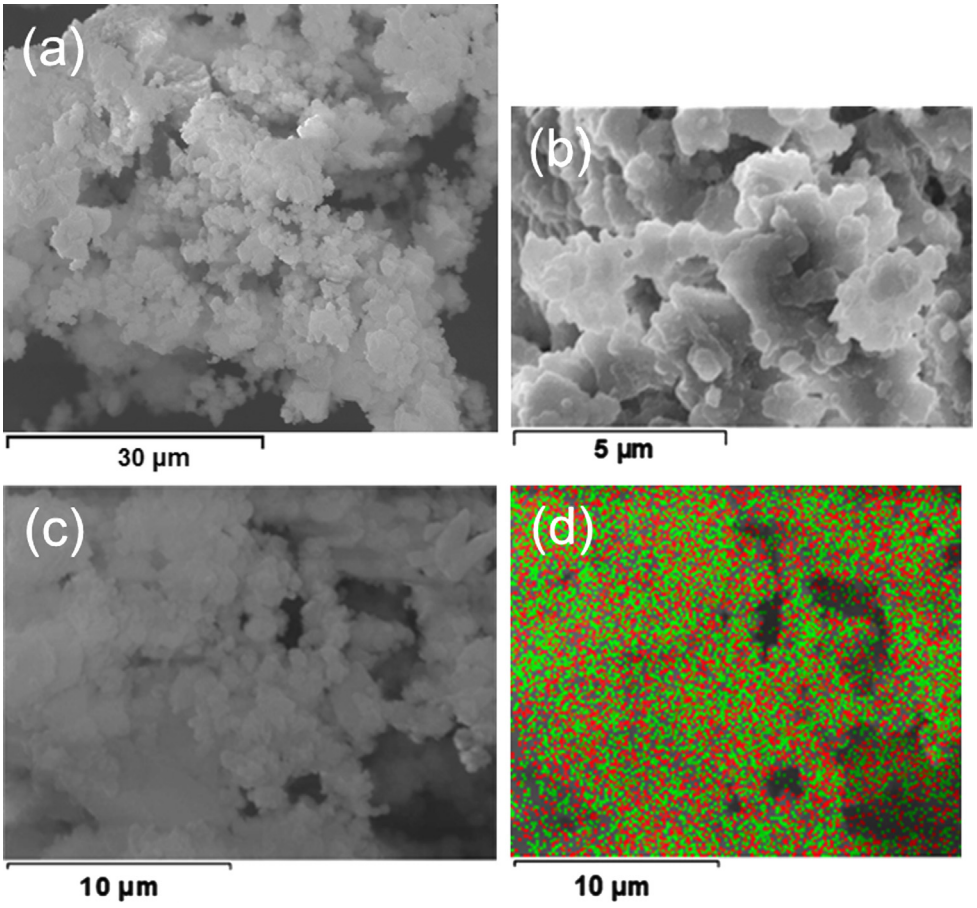

Fig. 2 SEM image of b:p 70:1 as-synthesised $NaMgH_3$ at (a) low magnification and (b) high magnification, and (c, d) morphology and elemental mapping of Na (red) and Mg (green) in the b:p 85:1 milled sample.

2. Experimental

All manipulations were performed in an Ar filled recirculating glovebox (Saffron Scientific, 1 ppm H_2O, 1 ppm O_2). Stoichiometric mixtures of anhydrous binary hydrides of NaH (Sigma-Aldrich, 95%; 0.2008 g) and MgH_2 (Alfa Aesar, 98%; 0.2198 g) were milled with stainless steel milling media (50 ml jar, 10 mm milling balls) under a nitrogen atmosphere at ambient conditions using a Retsch PM100 planetary ball mill. Ball:powder mass ratios (*b*:*p*) of approximately 70:1, 85:1 and 100:1 were employed using a total mill time of 5 h. Samples were milled at 450 rpm for 5 min periods with 5 min rest intervals between each mill. The synthesis of the ternary hydride was studied over 1–5 h of milling using the 70:1 ball:powder ratio to establish how the phase develops over time.

TPD experiments were performed *via* thermogravimetric–differential thermal analysis–mass spectrometry (TGA–DTA–MS; Netzsch STA 409 coupled to a Hiden HPR20 mass spectrometer). All thermal analysis experiments were conducted within an Ar-filled recirculating glovebox (MBraun UniLab; 0.1 ppm H_2O, 0.1 ppm O_2) using alumina sample pans under a constant flow of Ar at a 5 K min^{-1} heating rate.

Post-milled and post-thermal analysis samples were investigated by PXD using a Bruker D8 powder diffractometer in transmission geometry with spinning sealed capillaries. Data were collected over $5 \leq 2\theta(\text{deg}) \leq 85$ for 1 h for initial characterisation and over $10 \leq 2\theta(\text{deg}) \leq 95$ for 14 h to obtain higher resolution, higher intensity data (for structure refinement). Samples were also exposed to air and analysed *in-situ* using a PANalytical XPERT Pro MPD diffractometer in Bragg–Brentano reflection geometry (Cu Kα1 radiation). Data were collected for 1 h initially in the $5 \leq 2\theta(\text{deg}) \leq 85$ range for phase determination. All collected diffraction patterns were compared to reference data in the ICDD (JCPS) database using the PANalytical High Score Plus Software package. Rietveld refinement for the 70:1 5 h sample was performed using GSAS/EXPGUI [34,35] with reference data obtained from the Inorganic Crystal Structure Database (ICSD) [36] and the previously published structure for $NaMgH_3$ (ICSD91795) as a starting model [20]. Background was modelled using function 1 within GSAS, a shifted Chebyschev function. Peak shapes were modelled using the Thompson–Cox–Hastings pseudo-Voigt function (function 2) with asymmetry also being taken into consideration. The unit cell parameters were varied, followed by the atomic parameters. Major peaks from $Mg(OH)_2$ and MgO impurity phases were broad and could not be adequately fitted and so these 2θ ranges were excluded from the refinement.

SEM–EDX experiments were performed at 20 keV under a nitrogen atmosphere using a Philips XL30 ESEM instrument equipped with an Oxford Instruments X-act spectrometer to determine particle morphology and elemental ratios. Samples were prepared on carbon tabs under an inert environment. Prior to visualisation, the samples were loaded in a sputter coater and coated with gold at 25 keV. They were then transferred to the SEM sample chamber. Although exposure of the samples to air was unavoidable during this analysis procedure, it was minimised as much as possible to obtain representative results of the non-hydrolysed/non-oxidised samples.

Raman spectroscopy was conducted at room temperature (Horiba LabRam HR confocal microscope; 325 nm UV laser, 100 μm aperture, 600 grooves/mm grating, Synapse CCD). Spectroscopic data for ternary magnesium hydrides are limited and herein we compare experimental spectra for $NaMgH_3$ principally to previously calculated vibrational data and tentatively assign vibrational bonding modes. Sealed glass capillaries were used to contain the sample and thereby prevent air/moisture exposure during spectroscopic analysis. Raman spectra were also collected (*ex-situ*) for samples following dehydrogenation in TPD experiments.

3. Results and discussion

Using a ball:powder ratio of 70:1, PXD showed that $NaMgH_3$ forms after only 1 h of milling and after 5 h the reaction to the ternary hydride was complete. Increased PXD peak widths for the ternary phase after a 5 h milling time indicated a significantly reduced average particle size. At the lower b:p ratios studied, the particle sizes were inferred to be similar to those from milling with a b:p ratio of 70:1, but conversion was not complete and significant binary hydride phases were observed *via* PXD. When the b:p ratio reached 100:1, PXD patterns revealed that products were largely amorphous. The identity of the ternary hydride was confirmed from PXD data by reference to the ICDD PDF (card no. 00-052-0873) [21]. The as-synthesised $NaMgH_3$ sample was extremely air-sensitive, changing colour immediately from brown to grey/white. It was evident from PXD experiments that samples were indeed acutely sensitive to air. Despite best efforts to minimise air exposure, poorly crystalline $Mg(OH)_2$ and MgO phases were frequently formed (Fig. 1). No crystalline sodium-containing impurity phases were observed. Longer term exposure to moist air revealed that after a few minutes of air exposure, powder samples would ignite rapidly upon agitation. PXD analysis showed MgO, NaOH, Mg and $Mg(OH)_2$ to be present in the air-exposed products.

Table 1 Diffraction data for $NaMgH_3$.

Sample	$NaMgH_3$; 70:1, 5 h
Chemical formula	$NaMgH_3$
Crystal system	Orthorhombic
Space group	*Pnma* (No. 62)
Z	4
a (Å)	5.437(2)
b (Å)	7.705(5)
c (Å)	5.477(2)
V (Å^3)	229.49(9)
Formula weight (g)	201.276
Calculated density, ρ_x (g cm^{-3})	1.456
Refinement parameters	40
Data points	5086
R_{wp}	2.21%
R_p	1.68%
χ^2	2.11

Table 2 Atomic parameters for $NaMgH_3$.

Atom	Site	*x*	*y*	*z*	$U_{iso} \times 100$ (Å^2)
Mg	4*b* (0,0,1/2)	0	0	1/2	5.9(4)
Na	4*c* (*x*,1/4,*z*)	0.004(1)	1/4	0.013 (1)	0.3(4)
H1	4*c* (*x*,1/4,*z*)	0.503[a]	1/4	0.093[a]	2.5[a]
H2	8*d* (*x*,*y*,*z*)	0.304[a]	0.065[a]	0.761[a]	2.5[a]

[a]Parameters fixed in the refinement process.

The Scherrer equation (Eq. 1) was applied to determine the approximate crystallite size, D (across well-defined reflections over a typical 2θ range of 30–50°) [37]. A value of 0.9 was used for the shape factor, K, since the particle morphology appeared approximately isotropic from SEM imaging (see below) [38]. To account for instrumental broadening an LaB_6 powder standard was used to correct the FWHM of the $NaMgH_3$ sample (Eq. (2)), where B is the experimentally observed FWHM and b is the FWHM of the standard:

$$D = \frac{K\lambda}{\beta \cos\theta} \quad (1)$$

where

$$\beta = B - b \quad (2)$$

From the above treatment, the average crystallite size (more precisely, the average size of the crystalline domain) was estimated to be 430 nm for the 70:1 b:p, 5 h sample. Fig. 2 shows SEM micrographs for this sample. Low magnification images (e.g. Fig. 2a) show that the milled particles have a narrow size distribution but that agglomeration occurs during milling (as is often characteristic for the method). Higher magnification images (Fig. 2b) demonstrated that samples ranged from ~100 nm across up to 1 μm in size (the latter for particle agglomerations). The directly imaged particles show dimensions comparable with that estimated by Scherrer analysis of PXD data. The results of elemental mapping by EDX are shown in Fig. 2(c) and (d) and show good dispersion of Na and Mg throughout the sample. EDX point scans yielded approximate 1:1 elemental ratios of Na:Mg. Both findings are thus consistent with the formation of $NaMgH_3$

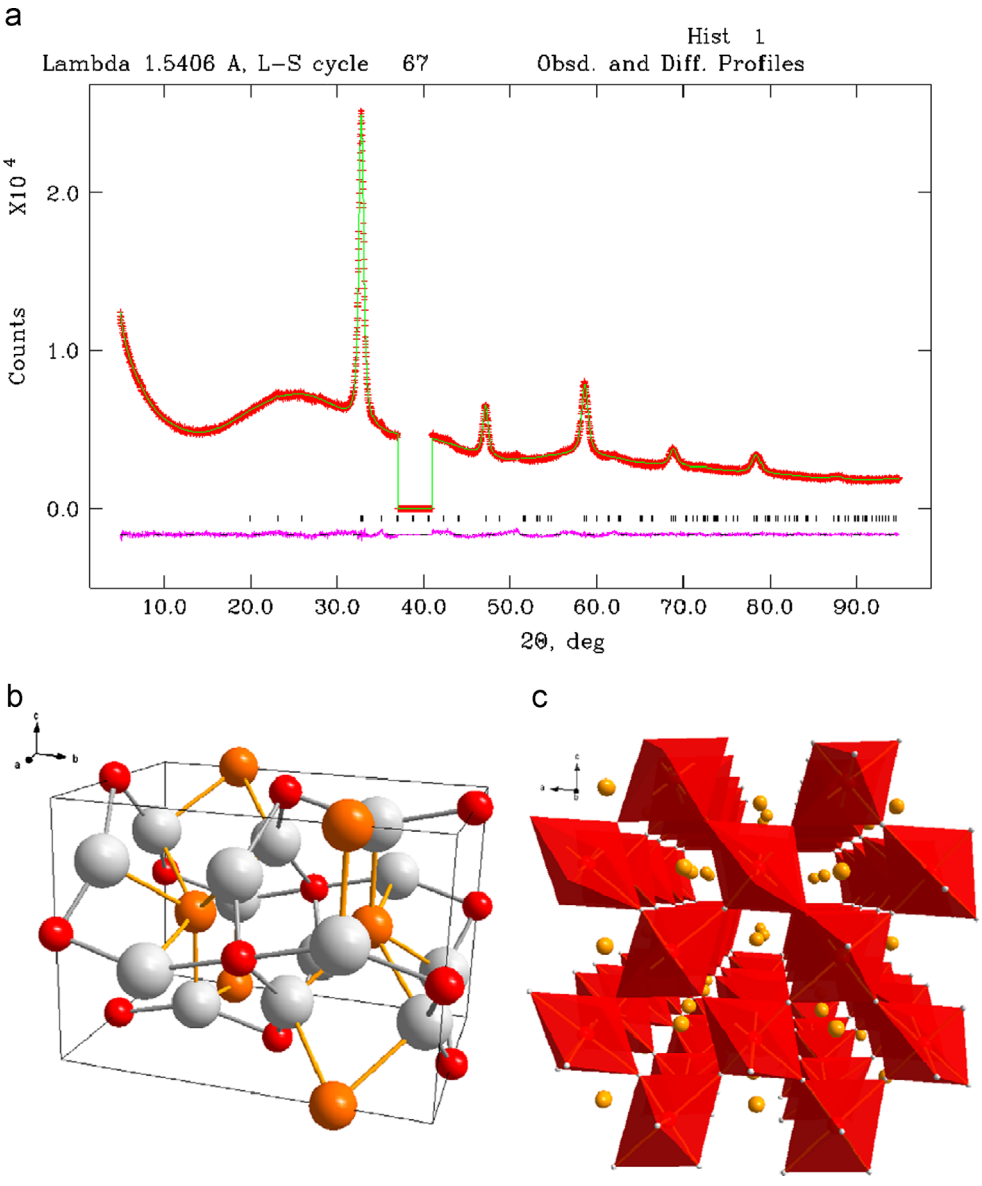

Fig. 3 (a) Rietveld refinement profile for $NaMgH_3$ (b:p 70:1, 5 h). (Observed data are shown by red crosses, the calculated plot is shown as a green continuous line, the tick marks indicate the reflection positions for orthorhombic $NaMgH_3$ and the difference plot is shown below in pink.) Major peaks from $Mg(OH)_2$ and MgO (see Fig. 1) were excluded from the refinement; (b) unit cell of $NaMgH_3$, where gold spheres = Na, red spheres = Mg and light grey spheres = H.; (c) extended structure of $NaMgH_3$ as a polyhedral representation viewed along the [010] direction. The red octahedra are centred by Mg.

and these results were obtained routinely for a number of b:p 70:1 and b:p 85:1, 5 h milled samples.

Rietveld refinement against PXD data was performed with an $NaMgH_3$ structural model based on that of Bouamrane et al. [20]. The refinement converged swiftly and smoothly to the previously reported orthorhombic perovskite structure (Tables 1 and 2). The Rietveld profile plot is shown in Fig. 3(a) and shows a good fit to the experimental data. Given the inability of PXD to locate light atoms accurately, the hydride positions were fixed as those from the starting model [20]. Considering the broad, undulating background in the PXD profile, it is quite possible that amorphous phases are also present in the milled material. From the data collected by Ikeda et al., it is also not possible to determine whether starting reagents or other impurities were contained in hydride products in their milling study, although the experimental weight loss they obtained on dehydrogenation (5.8 wt% vs. 6.0 wt% theoretically) would suggest that any such phases were not substantial [19]. The lattice parameters for the sample in this study are in reasonable agreement with those previously reported ($a=5.463$ Å, $b=7.703$ Å, and $c=5.411$ Å) [20], although, notably, despite a cell volume within 3σ of the previous value, the *a*-parameter and *c*-parameter are smaller and larger respectively in our work. (It is also worth noting that the cell volume is significantly larger than that of the corresponding deuteride [22].) Fig. 3(b) and (c) shows representations of the $GdFeO_3$ perovskite-type structure of the ternary hydride. The $GdFeO_3$ structure is well known and the details of the structure of $NaMgH_3$ are discussed in detail in previous publications [20–22]. As in previous literature models, the Na cations are surrounded by 12 hydride anions and Mg cations are coordinated octahedrally to 6 H^- anions.

The $NaMgH_3$ sample was observed to be acutely sensitive to the 532 nm (visible) laser when collecting Raman spectroscopy data and fluorescence effects were evident in spectra. Raman analysis was therefore conducted using (UV) laser irradiation at 352 nm (Fig. 4). To the best of the authors' knowledge, there are no previous experimental Raman spectra for $NaMgH_3$ in the literature. IR and Raman bonding mode symmetries and frequencies have been calculated computationally in two separate studies previously [24,32]. Our experimental data is in broad agreement with these studies allowing us to make a tentative assignment of the experimental spectrum (Table 3). Shifts at low wavenumber

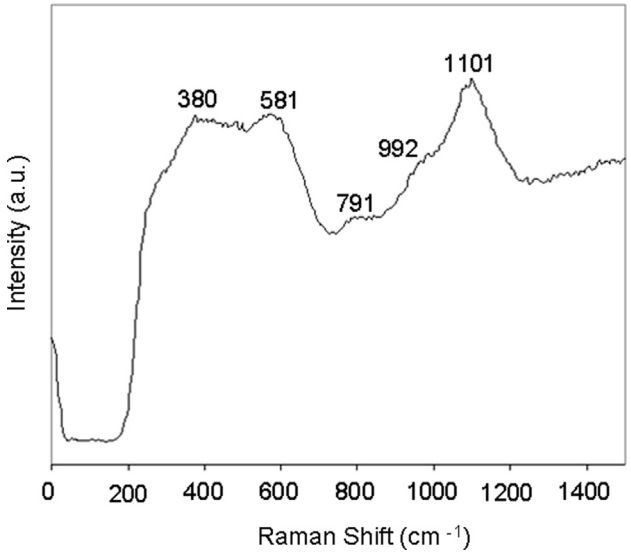

Fig. 4 Raman spectrum of $NaMgH_3$ (b:p 70:1, 5 h) collected using UV laser (325.1 nm) radiation.

Table 3 Assignment of the Raman spectrum for $NaMgH_3$ (b:p 70:1, 5 h).

Raman shift (cm^{-1})	Expected symmetry	Tentative assignment
380	B_{1g}	MgH_6 octahedral tilt
581	B_{3g}	δ, H–Mg–H
791	B_{3g}	δ, H–Mg–H
992	A_g	δ, H–Mg–H
1101	B_{1g}	ν_s Mg–H symmetric stretch

(380 cm^{-1}) indicate tilting/rotation of the MgH_6 octahedra, whereas the bands at 581 cm^{-1}, 791 cm^{-1} and 992 cm^{-1} suggest H–Mg–H angle distortions. In fact, the broad band at 992 cm^{-1} might represent a merging of two A*g* bands calculated by Bouhadda et al. at 906.8 cm^{-1} and 1071.4 cm^{-1} [30]. The band at 1101 cm^{-1} is in the Mg–H bond mode region and has been assigned to the symmetric Mg–H stretch. This assignment is again consistent with the bands calculated by Bouhadda et al. Data collected for samples milled for shorter durations (1 and 2 h of milling) did not show developed bands at higher Raman shift values, i.e., 700–1300 cm^{-1}, although the broad overlapping band between 200 and 700 cm^{-1} is evident. Spectra for samples milled at ball:powder ratios of 70:1 and 85:1 for 5 h are very similar in most respects, although the bands between 700 and 1300 cm^{-1} diminish again at the 100:1 ball:powder ratio, which may be the result of increased amorphisation and hence disorder within the sample milled at higher energy. (Additional Raman spectra are included in the supplementary information.)

The TPD data determined for $NaMgH_3$ (b:p 70:1, 5 h) are given in Fig. 5 and Table 4. Analysis of the DTA profile showed concurrent thermal events over the weight loss period corresponding to a two-step decomposition of the ternary hydride with concomitant hydrogen evolution as confirmed by MS. The onset temperatures of the two reaction steps (Eqs. (3) and (4); Table 4) could be determined from both the DTA and d(TG)/d*T* profiles, where the latter are omitted for clarity. Very similar thermal profiles were found for $NaMgH_3$ samples prepared at lower b:p ratios; although given that some starting reagents were evident from the PXD data for these samples, the second endothermic decomposition step was observed as broader and more pronounced. The desorption mechanism described by Ikeda et al. is given in Eqs. (3) and (4), where two losses of hydrogen are ascribed to the decomposition of $NaMgH_3$ and NaH respectively (Table 4) [19,25,26]:

$$NaMgH_3 \rightarrow NaH + Mg + H_2 \quad (3)$$

$$NaH + Mg + H_2 \rightarrow Na + Mg + (3/2)H_2 \quad (4)$$

The mass loss in the first step of the process (and therefore the total mass loss) associated with hydrogen release is significantly diminished with respect to that determined by Ikeda et al. and that expected theoretically. Our data indicate that hydrogen may be lost during the milling process, either pre- or post-reaction to form the ternary hydride (i.e. either *via* likely decomposition of the MgH_2 starting material or *via* the first step of the dehydrogenation of the ternary halide itself (Eq. (3))). Further evidence for this premise exists in the PXD patterns, where evidently Mg and/or MgH_2 in the milled products reacts rapidly with air during handling to form the respective binary hydroxide ($Mg(OH)_2$) and oxide (MgO).

Milling under elevated hydrogen pressure, therefore, may be one way in which this initial hydrogen loss may be prevented (although in subsequent rehydrogenation–dehydrogenation cycles the initial loss is not likely to be important unless phases react with air). PXD analysis of post-TPD samples revealed Na and Mg metal accompanied by MgO and NaOH (likely to be a result of the extreme air-sensitivity of the samples despite best efforts to minimise exposure during analysis). Crucially, no hydride phases were identified therefore suggesting that complete dehydrogenation of $NaMgH_3$ occurs by 723 K.

From Fig. 5 and Table 4, the onset temperature of the first dehydrogenation step is significantly lower than the equivalent temperatures for both the component binary hydrides. By comparison of the DTA profile of $NaMgH_3$ with those of the respective component binary hydrides, it is evident that the second hydrogen loss is associated with NaH decomposition. The onset temperature for hydrogen loss as determined by d(TG)/dT and corresponding mass spectroscopy data are lower than those previously recorded for $NaMgH_3$ by Pottmaier et al. This depression in temperature can be regarded in terms of particle size reduction (as a result of milling) and as a function of hydrogen partial pressure (Pottmaier et al. observed from DSC measurements that the onset temperatures decreased as the hydrogen pressure was reduced) [24].

The dehydrogenation enthalpies and entropies of $NaMgH_3$ have been studied by both computational and experimental means (Table 5). Our TPD data confirm that desorption proceeds *via* two endothermic steps, even when the ternary hydride is prepared in an inert environment. Further studies to demonstrate the effect our preparation method has on cycling and the enthalpy and entropy of dehydrogenation will be published in a later work. The ability to simplify the synthesis and processing of $NaMgH_3$ plus the prospect of tuning the kinetics and thermodynamics of hydrogen uptake and release, offer the potential both to develop $NaMgH_3$ as a storage system in its own right and to implement the ternary hydride as part of a "composite" approach (as recently demonstrated with NH_3BH_3, for example) [39].

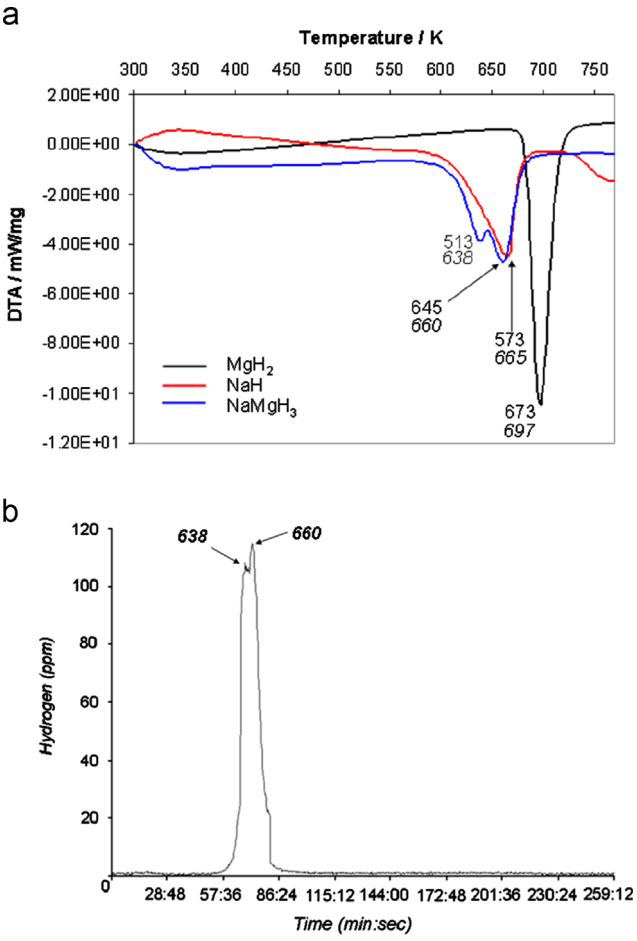

Fig. 5 (a) DTA data comparison for un-milled binary hydrides NaH and MgH_2 and ternary hydride, $NaMgH_3$ (b:p 70:1, 5 h). Values shown on profiles indicate onset and peak H_2 desorption temperatures, T_{onset} and T_{peak} respectively. (b) MS data for the $NaMgH_3$ (b:p 70:1, 5 h) indicate two overlapped hydrogen losses (T_{peak} values indicated on plot).

4. Conclusions

$NaMgH_3$ has been synthesised *via* mechanochemical methods under an inert atmosphere. The milled materials are nanocrystalline and the crystal structure of the ternary hydride is consistent with previous crystallographic data. Avoiding the use of high pressure sintering techniques is of significant importance for the facile preparation of hydrogen storage materials. Furthermore, synthesis in this way minimises the particle sizes, which has been shown to improve not only hydrogen desorption kinetics but also thermodynamics (e.g. in MgH_2). High ball:powder ratios are essential to ensure complete reaction to the ternary hydride (without milling under hydrogen). However, if this ratio is taken above a critical value, the ternary product loses crystallinity over similar milling times. The onset of weight loss and hydrogen evolution in mechanochemically synthesised $NaMgH_3$ occurred at lower temperatures than previously reported, although otherwise the two-step dehydrogenation proceeds as has been observed

Table 4 TGA–DTA–MS results for $NaMgH_3$ (*b:p* 70:1, 5 h) compared with literature data.

Event	Theoretical	This work		Ikeda et al. [19]		Pottmaier et al. [24][b]	
	H_2 (wt%)	T_{onset}[a] (K)	H_2 (wt%)	T_{onset} (K)	H_2 (wt%)	T_{onset} (K)	H_2 (wt%)
Step 1	4.0	513	2.67	–	–	664	–
Step 2	2.0	645	2.04	–	–	709	–
(Total)	6.0	–	(4.71)	–	(5.8)	–	–

[a]Temperature of weight loss onset.
[b]H_2 desorption onset temperatures determined by HP-DSC at 0.1 MPa H_2.

Table 5 Experimentally determined enthalpy and entropy for dehydrogenation of $NaMgH_3$ (modified from Supplementary material in Ref. [23]).

Process	H_2 ΔH (kJ mol^{-1})	H_2 ΔS (J K^{-1} mol^{-1})	Reference
Step 1	+88	–	[19,26]
$NaMgH_3 \rightarrow NaH+Mg+H_2$	+93.9	+116.2	[25]
	+94	+140	[14]
	+86.6	+132.2	[23]
	+92	+123	[24]
Step 2	+114.1	–	[19]
$NaH+Mg+H_2 \rightarrow Na+Mg+(3/2)H_2$	+102.2	+125.9	[25]
	+116	+165	[14]

previously. Inert mechanosynthesis techniques should offer considerable opportunity in the preparation of other ternary and higher hydrides.

Acknowledgements

DHG thanks the EPSRC for funding under Grants EP/E040071/1 and EP/I022570/1, the EPSRC, the Materials KTN and EADS Innovation Works for a CASE studentship for HR and the British Council for funding the placement of NM under the UK IAESTE Scheme.

References

[1] F. Cheng, Z. Tao, J. Liang, J. Chen, Chemical Communications 48 (2012) 7334.
[2] K. Yvon, Complex transition metal hydrides, Chimia 52 (1998) 613.
[3] K. Yvon and G. Renaudin, Hydrides: solid state transition metal complexes, Encyclopaedia of Inorganic Chemistry, vol. III, pp. 1814–1846.
[4] C.C. Koch, J.D. Wittenberger, Mechanical milling/alloying of intermetallics, Intermetallics 4 (1996) 339.
[5] A. Zaluska, L. Zaluska, J.O. Strom-Olsen, Nanocrystalline magnesium for hydrogen storage, Journal of Alloys and Compounds 288 (1999) 217.
[6] J. Huot, G. Liang, R. Schulz, Mechanically alloyed metal hydride systems, Applied Physics A72 (2001) 187.
[7] W. Bronger, Synthesis and structure of new metal hydrides, Journal of Alloys and Compounds 229 (1995) 1.
[8] A. Zaluska, L. Zaluska, J.O. Strom-Olsen, Structures, catalysis and atomic reactions on the nano-scale: a systematic approach to metal hydrides for hydrogen storage, Applied Physics A72 (2001) 157.
[9] P. Vajeeston, P. Ravindran, A. Kjekshus, H. Fjellvåg, First-principles investigations of the $MMgH_3$ (M=Li, Na, K, Rb, Cs) series, Journal of Alloys and Compounds 450 (2008) 327.
[10] D. Li, T. Zhang, S. Yang, Z. Tao, J. Chen, *Ab initio* investigation of structures, electronic and thermodynamic properties for Li–Mg–H ternary system, Journal of Alloys and Compounds 509 (2011) 8228.
[11] J.P. Bastide, A. Bouamrane, P. Claudy, J.M. Eltoffe, Elaboration d'hydrures doubles de magnesium et de potassium par réaction entre solides, Journal of the Less Common Metals 136 (1987) L1.
[12] R. Schumacher, A. Weiss, $KMgH_3$ single crystals by synthesis from the elements, Journal of the Less Common Metals 163 (1990) 179.
[13] B. Bertheville, T. Herrmannsdörfer, K. Yvon, Structures data for K_2MgH_4 and Rb_2CaH_4 and comparison with hydride and fluoride analogues, Journal of Alloys and Compounds 325 (2001) L13.
[14] K. Komiya, N. Moridaku, R. Rong, Y. Takahashi, Y. Shinzato, H. Yukawa, M. Moringa, Synthesis and decomposition of perovskite-type hydrides, $MMgH_3$ (M=Na, K, Rb), Journal of Alloys and Compounds 453 (2008) 157.
[15] M.A. Ghebouli, B. Ghebouli, A. Bouhemadou, M. Fatmi, S. Bin-Omran, Structural, elastic, electronic, optical and thermodynamic properties of $KMgH_3$, Solid State Sciences 13 (2011) 647.
[16] M. Fornari, A. Subedi, D.J. Singh, Structure and dynamics of perovskite hydrides $AMgH_3$ (A=Na, K, Rb) in relation to the corresponding fluorides: A first principles study, Physical Review B 76 (2007) 214118.
[17] A.H. Reshak, M.Y. Shalaginov, Y. Saeed, I.V. Kityk, S. Auluck, First-principles calculations of structural, elastic, electronic, and optical properties of perovskite-type $KMgH_3$ crystals: novel hydrogen storage material, Journal of Physical Chemistry B 115 (2011) 2836.
[18] Y. Bouhadda, N. Kheloufi, A. Betabet, Y. Doudouma, N. Fenineche, K. Benyalloul, Thermodynamic functions from lattice dynamic of $KMgH_3$ for hydrogen storage applications, Journal of Alloys and Compounds 509 (2011) 8994.
[19] K. Ikeda, Y. Kogure, Y. Nakamori, S. Orimo, Reversible hydriding and dehydriding reactions of perovskite-type hydride $NaMgH_3$, Scripta Materialia 53 (2005) 319.
[20] A. Bouamrane, J.P. Laval, J.-P. Soulie, J.P. Bastide, Structural characterisation of $NaMgH_2F$ and $NaMgH_3$, Materials Research Bulletin 35 (2000) 545.
[21] E. Rönnebro, D. Noréus, K. Kadir, A. Reiser, B. Bogdanovic, Investigation of the perovskite related structures of $NaMgH_3$, $NaMgF_3$ and Na_3AlH_6, Journal of Alloys and Compounds 299 (2000) 101.
[22] H. Wu, W. Zhou, T.J. Udovic, J.J. Rush and T. Yildirim, Crystal chemistry of perovskite-type hydride $NaMgH_3$: implications for hydrogen storage, Chemistry of Materials vol. 20, pp. 2335.
[23] D.A. Sheppard, M. Paskevicius, C.E. Buckley, Thermodynamics of hydrogen desorption from $NaMgH_3$ and its application as a solar heat storage medium, Chemistry of Materials 23 (2011) 4298.
[24] D. Pottmaier, E.R. Pinatel, J.G. Vitello, S. Garroni, M. Orlova, M.D. Baro, G.B.M. Vaughan, M. Fichtner, W. Lohstroh, M. Baricco, Structure and thermodynamic properties of the $NaMgH_3$ perovskite: a comprehensive study, Chemistry of Materials 23 (2011) 2317.
[25] K. Ikeda, S. Kato, Y. Shinzato, N. Okuda, Y. Nakamori, A. Kitano, H. Yukawa, M. Morinaga, S. Orimo, Thermodynamical stability and electronic structure of a perovskite-type hydride, $NaMgH_3$, Journal of Alloys and Compounds 446–47 (2007) 162–165.
[26] K. Ikeda, Y. Nakamori, S. Orimo, Formation ability of the perovskite-type structure in $Li_xNa_{1-x}MgH_3$ (x=0, 0.5 and 1.0), Acta Materialia 53 (2005) 3453.
[27] Y. Li, B.K. Rao, T. McMullen, P. Jena, P.K. Khowash, Electronic structure of the $LiMgH_3$ class of compounds: cluster calculations, Physical Review B 44 (1991) 6030.
[28] P.K. Khowash, B.K. Roa, T. McMullen, P. Jena, Electronic structure of light metal hydrides, Physical Review B 55 (1997) 1454.
[29] S. Hao, D.S. Sholl, Hydrogen diffusion in MgH_2 and $NaMgH_3$ via concerted motions of charged defects, Applied Physics Letters 93 (2008) 251901.
[30] Y. Bouhadda, Y. Boudouma, N. Fenineche, A. Bentabet, Ab initio calculations study of the electronic, optical and thermodynamic

properties of $NaMgH_3$, for hydrogen storage, Journal of Physics and Chemistry of Solids 71 (2010) 1264.
[31] S. Hao, D.S. Sholl, Role of Schottky defects in hydrogen and metal diffusion in NaH, MgH_2 and $NaMgH_3$, Journal of Physical Chemistry Letters 1 (2010) 2968.
[32] Y. Bouhadda, N. Fenineche, Y. Boudouma, Hydrogen storage: lattice dynamics of orthorhombic $NaMgH_3$, Physica B 406 (2011) 1000.
[33] A. Klaveness, O. Swang, H. Fjellvåg, Formation enthalpies of $NaMgH_3$ and $KMgH_3$: a computational study, Europhysics Letters 76 (2006) 285.
[34] A.C. Larson, R.B. von Dreele, General Structure Analysis System (GSAS), Los Alamos National Laboratory Report LAUR, pp. 86–748, Los Alamos, NM, USA, 1995.
[35] B.H. Toby, EXPGUI, a graphical user interface for GSAS, Journal of Applied Crystallography 34 (2001) 210.
[36] Inorganic Crystallographic Structure Database, ⟨http://cds.dl.ac.uk/⟩, (accessed 05.09.12).
[37] H.P. Klug, L.E. Alexander, X-ray Diffraction Procedures for Polycrystalline and Amorphous Materials, J. Wiley & Sons, New York, 1959.
[38] J.I. Langford, A.J.C. Wilson, Scherrer after sixty years: a survey and some new results in the determination of crystallite size, Journal of Applied Crystallography 11 (1978) 102.
[39] X.-D. Kang, J.-H. Luo, P. Wang, Efficient and highly rapid hydrogen release from ball-milled $3NH_3BH_3/MMgH_3$ (M=Na, K, Rb) mixtures at low temperatures, International Journal of Hydrogen Energy 37 (2012) 4259.